A synchrotron X-ray diffraction study of the structural phase behaviour of multilayer xenon on single-crystal graphite

1993 J. Phys.: Condens. Matter 5 8159

(http://iopscience.iop.org/0953-8984/5/44/009)

J. Phys.: Condens. Matter 5 (1993) 8159–8176. Printed in the UK

A synchrotron x-ray diffraction study of the structural phase behaviour of multilayer xenon on single-crystal graphite

W J Nuttall†§, K P Fahey†, M J Young†, B Keimer†¶, R J Birgeneau† and H Suematsu‡

† Department of Physics and Research Laboratory of Electronics, Massachusetts Institute of Technology, Cambridge, MA02139, USA

‡ Department of Physics, University of Tokyo, Tokyo, Japan

Received 14 June 1993, in final form 26 August 1993

Abstract. We present a high-resolution synchrotron x-ray diffraction study of xenon adsorbed on single-crystal graphite for coverages of two, three and six monolayers. We observe the evolution of the lattice mismatch between the xenon overlayer and a $\sqrt{3}\times\sqrt{3}R30°$ structure commensurate with the underlying substrate. In the case of the bilayer we see a first-order incommensurate–commensurate (IC–C) phase transition at 62.0 K ± 1.2 K, which we demonstrate is consistent with the layer closest to the substrate having locked into the commensurate sites. The role of substrate quality is discussed and we conclude that previous studies on relatively poorer substrates may have favoured equilibrium structures strongly influenced by the surface imperfections. The risk of an insufficiently equilibrated adsorbate is discussed in the context of the very slow kinetics we observe for multilayer xenon on high-quality substrates. For the three- and six-layer adsorbates we observe a systematic increase in lattice mismatch with film thickness and no indication of an incommensurate–commensurate transition. We conclude that the trilayer system consists of many distinct domains approximately 500 Å across, each of which has a random close packed structure.

1. Introduction

The extremely rich physics manifested in monolayer films of the noble gases on graphite substrates has been a topic of intense research activity for the last decade or so [1]. The physics of macroscopic crystals of these materials has also been investigated over this period, albeit less widely. The intervening regime between the effectively two-dimensional monolayer phase and three-dimensional bulk crystals has, however, been less extensively studied.

In this paper we report the results of a high-resolution synchrotron x-ray diffraction study of xenon multilayers on a high-quality single-crystal substrate. Graphite has a very large in plane thermal conductivity ensuring rapid thermal equilibration of the substrate, its basal surfaces are free of dangling covalent bonds, and its absolute heat of adsorption is large, being ~ 1900 K (164 meV) in the case of xenon [1].

Xenon on graphite is a system of particular interest to condensed matter investigators given the closely competing interactions that determine the behaviour of the xenon adsorbate. The competing interactions originate not from the absolute heat of adsorption but from the periodic ripple in this value that corresponds to the hexagonal electron distribution,

§ Current address: University of Keele, Keele, Staffordshire ST5 5BG, UK.

¶ Current address: Princeton University, Princeton, NJ 08544, USA.

0953-8984/93/448159+18$07.50

principally of carbon's delocalized p orbitals. This periodicity has an amplitude of only $\sim 61 \pm 3$ K (5.3 ± 0.3 meV) [2]. The pairwise Van der Waals' xenon–xenon interaction is of magnitude ~ 232 K (20.0 meV). In addition, the natural Xe–Xe bond length in a bulk crystal of face centred cubic (FCC) xenon is 4.384 Å at 58 K [3], whereas the length between the possible commensurate (C) sites in the graphite surface lattice is closely similar, being 4.254 Å at room temperature. These C sites form a lattice whose unit cell has linear dimensions $\sqrt{3}$ times larger than that of the underlying graphite substrate. The overlayer unit cell is also rotated by 30° with respect to the substrate and we shall adopt a Woods' notation $(\sqrt{3} \times \sqrt{3}R30°)$ to describe the C sites. The reciprocal lattice vector Q_C, corresponding to these C sites has a magnitude given by $2\pi/(4.254 \cos 30°) = 1.7055$ Å^{-1}.

It is now well established that monolayer xenon has a low-temperature C $(\sqrt{3} \times \sqrt{3}R30°)$ phase below ~ 65 K [4,5]. The intensive experimental investigation of monolayer rare gases adsorbed on graphite has been accompanied and motivated by a series of important theoretical developments.

Theoretical work into the nature of incommensurate (IC)–C transitions for rare gases (xenon and krypton) on graphite have largely concentrated on the role of domain boundaries in the behaviour of adsorbed IC monolayers. In examining the C–IC transition for monolayer krypton on graphite Villain demonstrated [6] that for a hexagonal domain system a first-order transition would be expected. Experiments reveal, however, that the krypton C–IC transition is observed to be, at a minimum, nearly second order [7]. In the case of monolayer xenon there is more consistent agreement between theory and experiment as a first-order transition is seen for a system with a hexagonal domain structure [5]. Further considerations of the role of domain walls for adsorbed rare gases at low temperature are given by Shrimpton *et al* [8] and Coppersmith *et al* [9]. Initial one-dimensional theoretical treatments of monolayer xenon predicted continuous transitions [10], but the incorporation of domain wall interactions in two dimensions suggested a first-order transition [11]. Renormalization group calculations incorporating an initial prefacing or restructuring stage have played a principal role in the development of the field and have generated comprehensive phase diagrams including first- and second-order transitions [11]. Theoretical work in the xenon on graphite system has largely been confined to the monolayer coverage region [12]. Despite the vast theoretical effort on the monolayer phase diagram and analysis by Bruinsma and Zangwill [13] of the behaviour of thick C multilayers there is at present no theoretical treatment for systems of thickness 2–10 monolayers.

In this paper we aim to elucidate the behaviour of multilayer films of xenon on graphite. Our experimental apparatus has been described elsewhere [14]. It allows us to perform high-resolution x-ray diffraction measurements on both single-crystal graphite and a vermicular powder ballast that is in thermodynamic equilibrium with the single crystal.

Previous studies of the structures of multilayer xenon have all been performed on substrates of relatively inferior quality. Our investigations have been performed on kish crystals of the highest quality, details of which are given in the next section. The best previous work is that of Hong and Birgeneau [15], which studied the adsorption of xenon multilayers on a natural single crystal of in plane mosaic $\sim 0.015°$ HWHM (half width at half maximum, as determined by supplementary studies at the National Synchrotron Light Source) and with an out of plane mosaic of $\sim 0.45°$ HWHM [14]. The relatively low resolution study of Hong and Birgeneau was performed on a rotating anode x-ray source. Hong and Birgeneau report that on cooling a first-order transition to a partial C phase occurs by ~ 55 K for a variety of multilayer films. Electron diffraction studies on xenon monolayers and bilayers have been reported by Hamichi *et al* [16].

The structure of this paper is organized into four sections. In section 2 we discuss

our synthetic single-crystal graphite substrates, the experimental sample cell and our method for determining xenon coverage. Section 2 is concluded with a discussion of the synchrotron x-ray diffraction techniques used. In section 3 we present our results. First we consider the behaviour of a xenon bilayer with decreasing temperature. We present detailed measurements of an IC–C transition in a xenon bilayer. We also probe the out of plane properties of the xenon structure and find evidence that the C component is a monolayer, presumably that closest to the substrate. We also present data for three- and six-layer xenon films for which no C phase is observed. We probe the out of plane structures of these multilayer films and we observe them to be randomly arranged close-packed layers. The paper is concluded in section 4.

2. Experiment

In order to gain accurate and useful experimental insights into the behaviour of multilayer films in a weakly modulated adsorption potential it is vital to have a substrate of optimal physical quality and chemical cleanliness. In our view, much of the observed behaviour of xenon multilayers is profoundly affected by substrate quality and difficulties arising from slow kinetics.

2.1. Substrate preparation

Our graphite substrates are known by the adjective 'kish', which refers to the smelting process by which they are prepared. They are generally small single crystals, approximately 2 mm × 1 mm × 50 μm, where the significant surfaces correspond to the exposed basal planes. The kish graphite crystals are formed, at $\sim$ 3000 °C, as a precipitate from a supersaturated iron solution, which forms as the iron gradually evaporates. The crystals are formed embedded in the iron, which is dissolved away using sulphuric acid. The final cleaning stage is to place the crystals in a stream of chlorine gas at 2500 °C.

For our synchrotron x-ray diffraction experiment we only used crystals with excellent surface morphology. The crystals employed were from batches verified by scanning Auger microscopy to be free of silicate contamination that can remain on the surfaces of the kish crystals despite the cleaning procedures described earlier. To confirm that the surface quality was indeed optimal we adsorbed a C monolayer of krypton and found that its correlation length was of the same order as our longitudinal resolution. This is shown in figure 1. In this paper we define our measure of real space length scales ξ as the reciprocal of the HWHM κ of a Lorentzian fit, $\xi = 1/\kappa$.

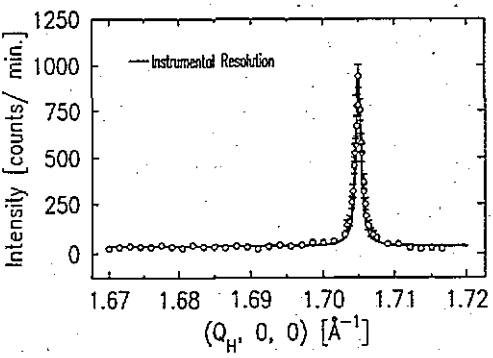

Figure 1. A longitudinal scan through a C krypton (10) peak at 90 K. These data were taken at beamline X20B just prior to the xenon bilayer experiment. Our instrumental resolution 0.0004 Å^{-1} (HWHM) is also shown to illustrate the exceptionally high quality of the crystallized krypton monolayer.

2.2. Sample cell assembly and coverage determination

In this experiment we shall make repeated reference to the xenon coverage or filling fraction which we denote by f and express in xenon monolayers (ML). The coverage f is determined by a volumetric thermodynamic measurement and is independent of our x-ray observations. In order to use volumetric means to control and determine the amounts of xenon condensed it is necessary to have a very large adsorbing graphite substrate. Our kish crystal is far too small to be able to make such measurements. We therefore place in the cell a ballast of vermicular graphite in thermodynamic equilibrium with the kish crystal. The kish crystal has a surface area of only about 3 mm^2 whereas the vermicular has a surface of 10 $m^2\ g^{-1}$. From the coverage of the krypton C–IC transition we calculate that for a typical charge of vermicular graphite we have an adsorbing surface of 1.3 m^2.

It is very important to ensure that both substrates are clean prior to the dosing of the xenon adsorbate. The vermicular ballast is baked to $\sim$ 700 °C in a quartz glass bake out tube which, by means of a turbo-molecular pump, is held at approximately 10^{-5} Torr. It is then transferred in a nitrogen atmosphere to the small ballast cell which is equipped with beryllium windows to allow x-ray studies. The ballast cell is allowed to be exposed to the atmosphere only for its final attachment to the mount of the carefully aligned kish crystal. The complete sample assembly is then sealed inside our high-vacuum beryllium can mounted on the cold finger of a closed cycle helium refrigerator.

The system is then baked to approximately 200 °C with the exception of the beryllium can which is not heated beyond 100 °C as it contains an indium seal. Typical room temperature base pressures are $\sim 1.0 \times 10^{-7}$ Torr falling to $\sim 5 \times 10^{-8}$ Torr on cooling. It is essential that the temperatures of the single crystal and the vermicular ballast are equal so as to ensure that the xenon adsorbate is at the same place in the phase diagram in each case. In order to ensure thermal homogeneity, all of our single-crystal data have been collected with an overpressure of 0.3–1.0 Torr of research purity (99.9993%) helium in the cell as a thermal mediator.

The actual phase behaviour of the xenon is a function of both the temperature and the substrate chemical potential of the adsorbate μ_A. In thermodynamic equilibrium the chemical potential of the adsorbate must equal that of the vapour μ_V

$$\mu_A = \mu_V \tag{1}$$

where the chemical potential of the vapour may be approximated by the ideal gas result

$$\mu_V = kT \ln (P\lambda^3/kT) \tag{2}$$

where λ is the thermal wavelength

$$\lambda = h/(2\pi mkT)^{1/2}.$$

One may therefore regard the thermodynamic variables of the phase space as (μ_A, T) or equivalently (P, T). If there were an inhomogeneity, one might imagine a larger number of layers condensed on one substrate rather than the other with all the concomitant uncertainties that would entail.

The experimental work presented here spans the temperature range of 95–45 K. Because of the structure of our cell, absolute temperatures are only known to $\pm$ 1 K while relative temperatures are accurate at the level of $\pm$ 0.1 K. In order for a phase space described in terms of temperature and coverage to be useful, it is important that the number of xenon layers does not itself vary strongly with temperature. Figure 2 shows a series of diffraction scans from xenon adsorbed onto a vermicular graphite ballast in our cell. These diffraction data clearly show that the multilayer regime for our investigation must be below $\sim$ 120 K.

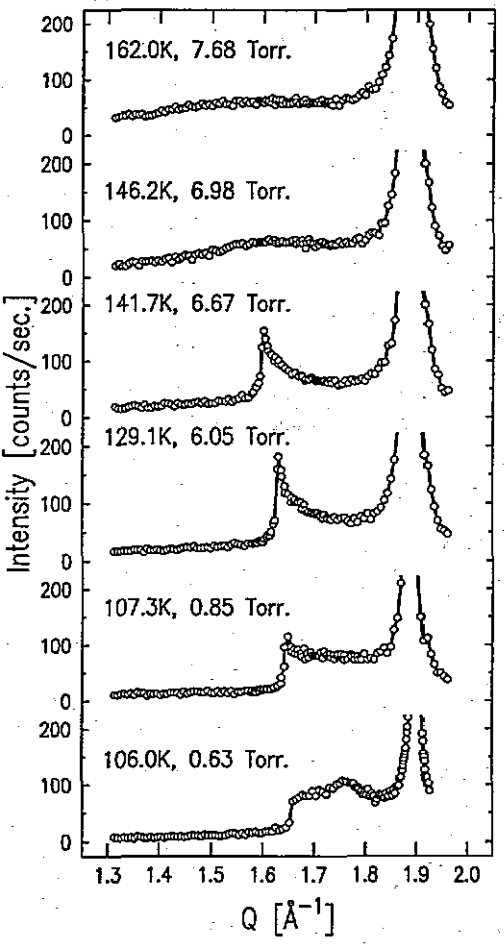

Figure 2. The growth of a multilayer of xenon on vermicular graphite. Scans are shown for a closed cell experiment with an $f = 3.1$ ML charge of xenon. Actual coverages were determined *in situ* by volumetric means to be: 0.70 ML at 162 K; 0.83 ML at 146 K; 0.91 ML at 142 K; 1.11 ML at 129 K; 2.79 ML at 107 K and 2.87 ML at 106 K. There is an ordering transition in the sub-monolayer regime between 146.2 K and 141.7 K revealed by the appearance of an asymmetric peak characteristic of an in plane ordered IC structure. As the temperature is cooled further the incommensurability of this monolayer feature decreases. At 107.3 K, however, we see evidence of a peak corresponding to pure out of plane multilayer structure. As the multilayer grows the (10) IC scattering rods modulate out of plane, which when powder averaged causes the peak to become less distinct.

Above $\sim$ 120 K the coverage f is a very strong function of temperature. At 95 K the partial overpressure of xenon is negligible compared to the original dosing pressures, that is, all of the admitted xenon has condensed. The quantity condensed is described by our measure f, which is essentially constant for 45 K $< T <$ 95 K.

Having accepted a volumetric definition of coverage f it is important to appreciate certain conditions that apply. First, in this experiment we shall be dealing principally with IC xenon structures of lower density than the C adsorption sites. This means that if the structure were indeed layered, the actual number of xenon layers would then be up to approximately 3% larger than the f value cited. This small discrepancy is itself temperature dependent as the xenon adsorbate contracts upon cooling, bringing the adsorbate closer to the C site density used to define f. Also, of course, our measure, f, makes no distinction whatsoever as to the nature of the xenon adsorption, be it layered or otherwise.

Previous studies of the multilayer xenon–graphite system [17,18] lead us to expect a layered structure, at least in the case of films of just a few layers, such as those considered here. We have no evidence in our data which leads us to doubt that conclusion.

2.3. Synchrotron x-ray diffraction

The data presented here were collected in three independent runs at IBM–MIT beamline X20-B of the National Synchrotron Light Source at Brookhaven National Laboratory. In each case the experimental configuration was the same. X20-B is a fixed energy (17.4 keV) horizontally focusing synchrotron beamline, which employs a bent Si(111) monochromator. For details of the beamline etc please refer to [19].

The only technical difference between the data runs was that the bilayer data were collected with an x-ray beam that had been reflected from a gold mirror. The mirror consists of a vertically mounted block of flat gold plated float glass, and it is mounted so as to be in a total external reflection condition for the principal 17.4 keV radiation but not the higher harmonics such as $\lambda/3$, which also satisfy the monochromator Bragg condition. The $\lambda/3$ is of particular interest as it generates a peak due to the bulk graphite (110) planes at the same spectrometer position as the $(Q_C, 0, 0)$ mid-point of a C $\sqrt{3} \times \sqrt{3}R30°$ adsorbate's scattering rod. In our later studies of the three- and the six-layer system we felt the small benefit provided by the mirror was outweighed by its disadvantages of lower flux, a more difficult sample alignment, and a more time consuming set-up procedure for the synchrotron beam itself. In the three- and six-layer data we found this spurious $\lambda/3$ peak to be only a mild inconvenience as we could simply cut the modulated scattering rod at a place slightly displaced out of plane and so avoid the discrete spot due to the bulk graphite $\lambda/3$ completely.

The closed cycle displex refrigerator housing the sample is mounted on a Huber six-circle goniometer in a vertical scattering geometry. Before the beam impinges on the sample we have a set of incoming slits which in a typical run would be set at 1.0 mm out of plane and 3.0 mm in plane. The outgoing resolution is determined in the out of plane direction by a pair of collimating slits. In plane, the resolution is defined by a germanium (111) analyser crystal. The resolution function is measured in the longitudinal direction Q_H using a silicon (111) face at the centre of rotation. Q_L resolution is determined from the bulk graphite substrate.

The resulting resolution ellipsoid has a longitudinal semi-minor axis (Q_H) 0.0004 Å^{-1} and a semi-major axis, out of plane, (Q_L) 0.0111 Å^{-1}. The graphite crystal is mounted with its basal surface aligned with the scattering plane for $Q_L = 0$. This geometry aligns the xenon scattering rod with the major axis of the resolution ellipsoid. As one scans up the rod, however, the resolution ellipsoid tilts with respect to the rod and a reduction in signal intensity is observed. This effect is illustrated schematically in figure 3.

3. Results

3.1. Bilayer behaviour

Our experiments studied xenon coverages of f = 2.05, 3.05 and 5.82 ML. In the case of the bilayer film we see clear evidence of a transition at 62 ± 1.2 K from an entirely IC structure to one with coexisting IC and C components. A set of representative scans from this evolving structure is shown in figure 4. This transition temperature is consistent with the observations of Hong [14] where he reports that, on cooling, a transition to a partial C phase occurs by ~ 55 K for a variety of multilayer films.

3.1.1. Kinetics and substrate quality. In figure 4 we notice that as the temperature is lowered the longitudinal width of the scattering peak broadens until at the point of the transition it corresponds to an effective longitudinal length scale ξ_H, of only 270 Å, which is an order of magnitude worse than the longitudinal resolution. It is unlikely that this spread in Q_H

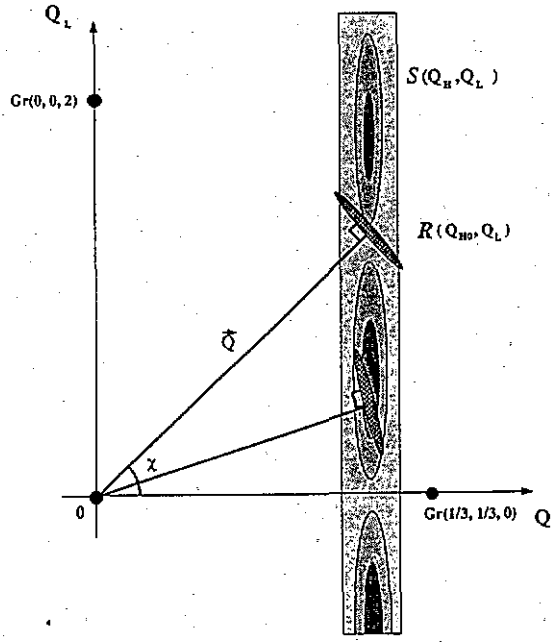

Figure 3. Illustration of the resolution geometry at various points along the Bragg rod. The xenon (10) scattering rod passes close to but is IC with respect to the graphite ($\frac{1}{3}$, $\frac{1}{3}$, 0) position, where in each case reference is made to the xenon or graphite's own lattices which are rotated by 30° with respect to each other.

is due to a thermal gradient on our sample given both its small size and the extremely good in plane thermal conductivity of the graphite single crystal. Rather, we believe that as the xenon compresses on cooling, a complex rearrangement of the atoms must occur as atoms are drawn in from the upper layers and the vapour. The possibilities for quenched disorder associated with pinned vacancies and domain wall structures provide a rational expectation that the in plane ξ_H of the multilayer will be reduced as we cool. Hamichi *et al* [20] also report a broadening of the xenon longitudinal IC signal in their electron diffraction experiment as the system is cooled. They suggest that this behaviour is related to a rearrangement of the dislocations within the grain boundaries while the dislocation density remains constant. They propose that the behaviour is representative of a clean, smooth, weakly modulated substrate in thermal equilibrium.

One might expect that the length scale ξ_H over which the adsorbate can be said to be ordered would depend strongly on imperfections of the graphite surface. The adsorption of the near perfect krypton C phase monolayer demonstrates that our graphite surface is defect free on a length scale an order of magnitude better than that observed in low-temperature xenon. We might expect, however, that far more time would be required in order to establish equilibrium across the large clean flat surfaces of these crystals. As we shall see below, this is in fact the case.

It should be noted that the cooling data run summarized in figure 5 was taken with care to cool the system extremely slowly. The growth in the C phase signal at 60 K was seen to occur gradually over an 8 h period. The first indications of a transition were evident quite rapidly, but the time evolving nature of the signal caused us to wait until we were confident that equilibrium had been re-established. In previous data runs in which the bilayer system had been cooled more rapidly we observed that we could effectively super-cool the IC bilayer system down to $\sim$ 50 K without any indication of an IC–C transition. The incommensurability's variation with temperature appeared to freeze out gradually. This suggested that we may have no longer been witnessing equilibrium

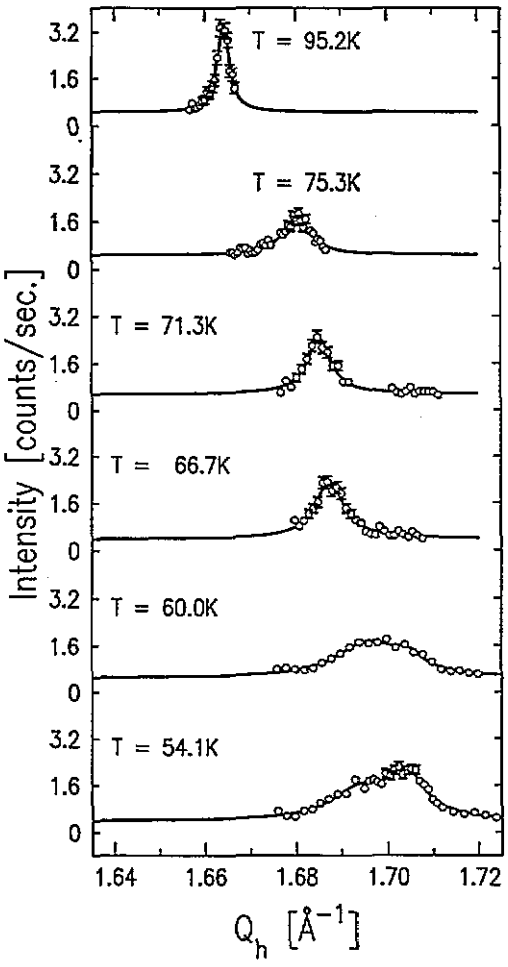

Figure 4. Longitudinal in plane scans from a 2.05 ML xenon adsorbate on a high-quality single-crystal substrate. The IC phase is seen to shift with decreasing temperature until a C phase signal at $Q_H = Q_C = 1.7055$ Å^{-1} appears at 62.0 ± 1.2 K.

behaviour and accordingly, the investigation was repeated more slowly, as has been shown in figure 5.

We observe that as the incommensurability of the xenon bilayer decreases, the width of the IC peak is seen to broaden. As can be seen from figure 6, the form of the interdependence between width and incommensurablity is given approximately by

$$\log_{10}(\delta Q/\kappa_H) \propto \delta Q. \tag{3}$$

Such behaviour has also been reported by Stephens *et al* [21] for monolayer krypton on a *ZYX* exfoliated graphite powder. In their experiment they observed that the IC–C transition occurred when the incommensurability of the krypton adsorbate was of the same magnitude as the longitudinal width

$$\delta Q/\kappa_H \simeq 1.$$

Our bilayer xenon film also undergoes an IC–C transition when the film reaches that regime. Stephens *et al* interpret their result to indicate that for a hexagonal network of domain walls, the walls are disordered on a length scale approximately equal to their separation.

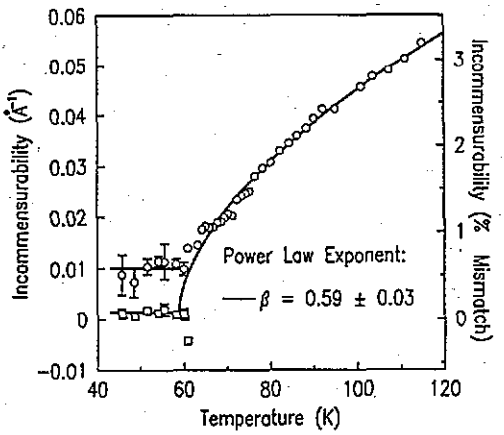

Figure 5. Temperature variation of the incommensurability ($Q_{IC} - Q_C$) for a xenon bilayer $f = 2.05$ ML. The IC peak position is represented by ○, while the C peak is denoted by □.

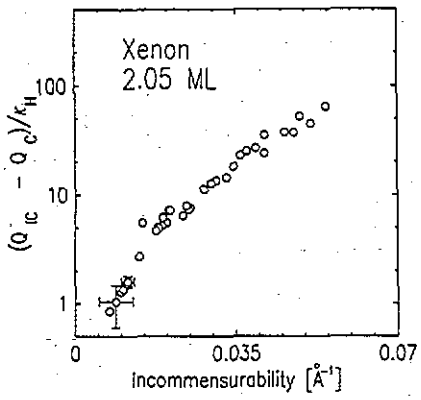

Figure 6. (Incommensurability/peak width) versus incommensurability. This figure illustrates the relationship of the ratio of the incommensurability of the peak to its width as function of temperature. A pair of representative error bars is shown at $Q_{IC} = 0.0088$ Å^{-1} and $Q_{IC} = 0.0115$ Å^{-1}. Above 0.0115 Å^{-1} errors are within the size of the points shown.

We believe that the behaviour that we have observed in our bilayer film represents either true equilibrium or very close to it. It seems likely, however, that the ambiguities originating from the very slow kinetics on these high-quality substrates will worsen as we go on to consider thicker multilayers. Thus one must be particularly aware that the thicker xenon multilayers may not be fully equilibrated.

3.1.2. Transverse and out of plane structure. The use of a single-crystal substrate allows a study of the transverse and out of plane behaviour of the xenon multilayer. In figure 7, we show representative Q_K scans, which provide structural information transverse to the longitudinal data in figure 4. The Q_H data in figure 7 are taken along a path in reciprocal space 60° away from that followed in the Q_H scan. It is, therefore, not a true transverse scan, but it will nonetheless contain transverse information. In figure 7 we observe that the transverse width of the IC xenon adsorbate peak is invariant with temperature. The C phase component peak, however, is seen to be significantly broader than either the IC transverse width or the longitudinal Q_H width of the C component peak as is determined from a two-Lorentzian fit to the coexisting IC and C phases. The width of our 45.7 K C phase Q_H component peak implies that the patches of C order are approximately 250 Å across. The poor transverse order implies a mosaic spread in the nominally C adlayer. The mosaic of the C phase xenon is significantly worse than the bulk mosaic of the substrate. Similar behaviour was also seen for the krypton monolayer.

Figure 5 summarizes the variation of the adlayer incommensurability with temperature. It is clear that there is a phase transition at $T = 62 \pm 1.2$ K to a $\sqrt{3} \times \sqrt{3}R30°$ C phase for at least part of the xenon adsorbate. Clearly one possibility is that the system has phase separated into domains two layers thick, some of which are IC by $\sim 0.5\%$ and some of which correspond to a uniform C bilayer. Alternatively, it could be that the layer nearest the graphite substrate has undergone a phase transition to a C structure while the layer above has remained IC. We hope to demonstrate the validity of the latter view.

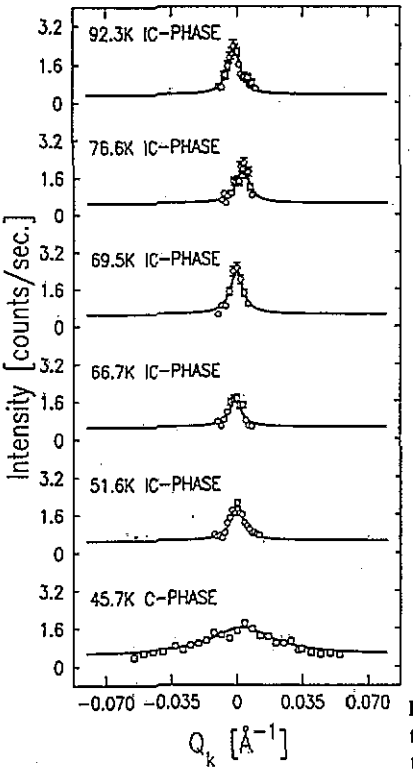

Figure 7. Q_K scans at 60° to the longitudinal Q_H data. This shows the transverse stability of the IC peak and the significantly broader transverse width of the C phase.

Angle resolved photo emission spectroscopy studies of bilayer xenon on graphite [22] report that at 44 K the xenon bilayer has a compressed C phase first layer and an uncompressed upper layer. It is reported, however, that the IC second layer has a d spacing close to that of bulk xenon. An electron diffraction experiment by Hamichi *et al* [20] did not observe a bilayer phase with a C component for 50 K $< T <$ 80 K. It is important to note, however, that a typical electron diffraction measurement is performed over a timescale of minutes rather than the hours which we determined were necessary for complete equilibrium in our x-ray diffraction studies.

In figure 5 we have shown a fit to the incommensurability of the IC component that corresponds to a power law dependence of the form

$$(Q_{IC} - Q_C) = (T - T_0)^{\beta}. \tag{4}$$

Our observed exponent ($\beta = 0.59 \pm 0.03$) does not agree with the results for monolayer rare gases on graphite or for the surfaces of noble metals where $\beta \simeq 0.33$ is observed [21,23,24]. This is not unexpected, however, given that the system itself may be changing in the immediate neighbourhood of the transition from a coupled bilayer to two independent monolayers. The slope of the incommensurability above the transition is almost linear and is consistent with a measure of the thermal expansivity of a xenon bilayer as being $= 4.62 \times 10^{-4}$ K^{-1} for $T > T_0$. As might be expected this is significantly larger than the thermal expansivity of bulk xenon over the same temperature range ($\sim 2.21 \times 10^{-4}$ K^{-1}) [25].

The out of plane structure of a multilayer film is particularly difficult to determine experimentally. The use of a single-crystal substrate, however, allows us to probe, for

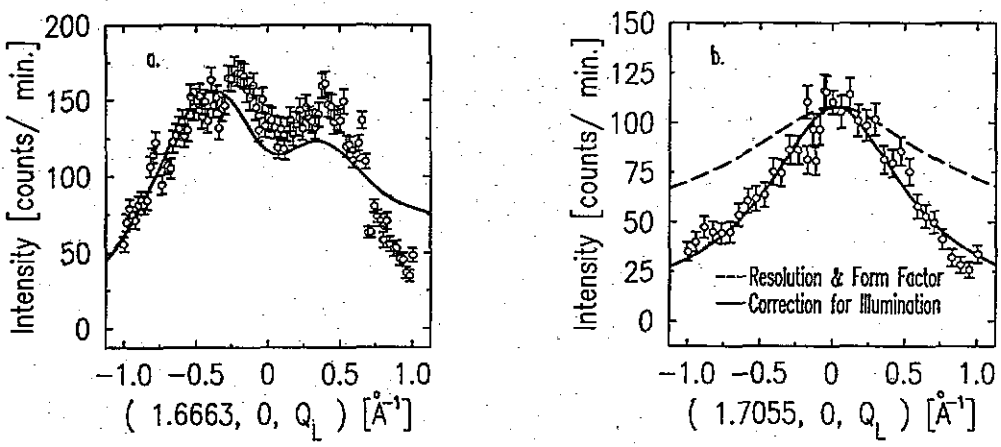

Figure 8. (a) Xe (Q_K, 0, Q_L) rod scan out of plane through the IC in plane peak at 75.4 K. The modulated profile of the scan suggests a multilayer structure to the adsorbate, where each layer has the same in plane periodicity and therefore incommensurability. The solid line corresponds to our expectations for a model structure that is 85% bilayer approximately evenly distributed between regions of AB and AC stacking. The remaining 15% of the surface has a trilayer stacking. An offset to the zero of Q_L of 0.11 Å^{-1} has been allowed for the fit. (b) Xe (Q_C, 0, Q_L) scan through the in plane C peak at 51.6 K. We note that the local minimum at $Q_L \approx 0$ has gone and the profile is as would be expected for a monolayer. This leads us to conclude that the C phase is one layer thick and the IC phase is also a monolayer at this temperature.

instance, the thickness of the C phase component of our $f = 2.05$ ML adsorbate. Four-circle x-ray diffraction is particularly useful in being able to obtain such information directly.

Figure 8 shows data from a scan of Q_L along the out of plane scattering rod. This scan was taken at $Q_K = 0$ and at a fixed Q_H, which we shall label Q_{H0}. This type of scan was discussed in some detail by Hong and Birgeneau [15]. The crystal orientation is the same as in the experiment of Hong and Birgeneau, with the long axis of the resolution ellipsoid aligned with the xenon scattering rods for $Q_L = 0$. As one scans up the rod of Bragg scattering the resolution ellipsoid tilts with respect to the scattering rod and therefore a reduced signal is seen. In figure 8(a) we see the out of plane structure factor for the IC system at 75.4 K. Figure 8(b) is, however, simpler in form and we shall consider this scan first. This shows the (Q_C, 0, Q_L) out of plane structure of the C part of the adsorbate at 46.4 K. The smoothly modulated profile of a single peak centred at $Q_L = 0$ has the qualitative features one would expect for a monolayer scattering rod. The dashed curves in figure 8 are the model profiles we would expect from our apparatus incorporating the resolution effect illustrated in figure 3. The only parameter being varied in this case is the peak amplitude. This profile is established by a two-dimensional convolution in the space of Q_H and Q_L

$$I(Q_H, Q_L) \propto \int\int \mathrm{d}q_l \mathrm{d}q_h \left(R[(q_h - Q_H), (q_l - Q_L)] \frac{1}{1 + (q_h - Q_{H0})^2/\kappa_H^2} \mid f_{Xe}(q_l) \mid^2 \right). \tag{5}$$

We convolve our resolution ellipsoid $R(Q_H, Q_L)$ with the xenon scattering rod, which is taken to have a Lorentzian cross section in the Q_H direction centred at Q_{H0}, and of width

κ_H. This is modulated out of plane by the xenon atomic form factor $f_{Xe}(Q_L)$ in the Q_L direction.

Although such a model profile does indeed have the qualitative features of the data it is clear that there is an additional effect involved that acts to diminish the observed signal at large Q_L. In order to generate the fit shown by the solid curve in figure 8(b) we have attempted to take account of this final important empirical effect. As we scan up and down the rod in Q_L the orientation of the crystal is adjusted with respect to the incoming beam, and as a result the effective illumination of the crystal is itself a function of Q_L. To take account of this effect we have introduced an *a posteriori* cosine decay $C(Q_L)$ to the signal. Including the form of our resolution ellipsoid $R(Q_H, Q_L)$, we have

$$I(Q_{H0}, Q_L) \propto \int\int \mathrm{d}q_l\,\mathrm{d}q_h \Bigg(\exp\Big\{ -\xi_x^2 \big[(q_h - Q_{H0}) \cos(\chi) + (q_l - Q_L) \sin(\chi) \big] - \xi_y^2 \big[(q_l - Q_{L0}) \cos(\chi) - (q_h - Q_H) \sin(\chi) \big] \Big\} \times \frac{1}{1 + (q_h - Q_{H0})^2/\kappa_H^2} \mid f_{Xe}(q_l) \mid^2 C(Q_L) \Bigg) \tag{6}$$

where

$$\sin(\chi) = Q_L/\left(Q_{H0}^2 + Q_L^2\right)^{1/2} \qquad \cos(\chi) = Q_{H0}/\left(Q_{H0}^2 + Q_L^2\right)^{1/2}. \tag{7}$$

The solid curve fitted to the data in figure 8(b) has two freely varying parameters, the amplitude and the rate of decay of the cosine effect. A small correction of 0.02 Å^{-1} to the zero of Q_L was also incorporated. This measure $C(Q_L)$ of the illumination effect, has been incorporated into all other fits to the $(Q_{H0}, 0, Q_L)$ data presented here. We fixed our scattering vector's azimuthal orientation by selecting an azimuthal vector (1, −2, 0) perpendicular to the (Q_H, Q_L) plane.

In figure 8(a) we show the profile of the Bragg rod observed for the IC $f = 2.05$ ML structure. Given that this structure is IC and of lower atomic density than the C coverage used to define $f = 1.0$ ML, the actual number of xenon layers present on the substrate at this temperature is actually somewhat higher, being 2.15 ML. That is, we assume that 85% of the surface is covered by an ordered xenon bilayer of either AB or AC stacking while the remaining 15% is a xenon trilayer of ABC, ACB, ABA or ACA stacking. We also expect that the inter-layer spacing of the xenon adsorbate will vary slightly with temperature. We observe from the in plane scattering vector that the presence of the substrate compresses the in plane xenon lattice relative to the periodicity of a bulk xenon crystal at that temperature. We therefore naively expect that the out of plane xenon spacing might increase so as to preserve the total unit cell volume. By this method we arrive at an estimate of the inter-layer spacing. The solid curve in figure 8(a) is the kind of profile that our apparatus would generate if the model structure we discussed were allowed to relax out of plane by a further 2.7% and if the bilayer component were 47.4% AB stacking. In this case the trilayer component is predominantly ABC stacking. We generate this lineshape by fitting with a package that fits to a sum of a bilayer and trilayer profile in appropriate proportion. The bilayer fit has the form

$$I(Q_{H0}, Q_L) \propto \int\int \mathrm{d}q_l\,\mathrm{d}q_h \Bigg(R\big[(q_h - Q_{H0}), (q_l - Q_L)\big] \frac{1}{1 + (q_h - Q_{H0})^2/\kappa_H^2} \mid f_{Xe}(q_l) \mid^2 \times \frac{1}{2}\big[S_{AB}(q_l) + S_{AC}(q_l)\big] C(Q_L) \Bigg) \tag{8}$$

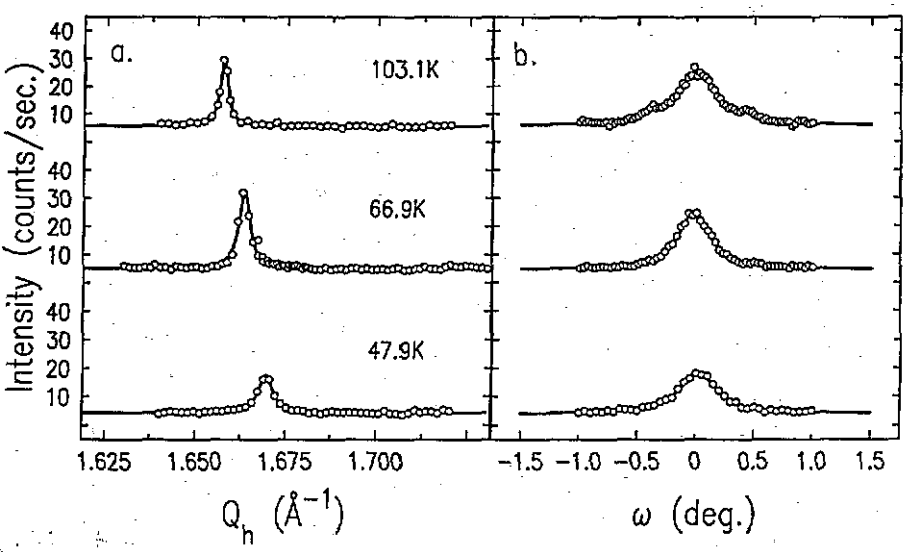

Figure 9. (a) In plane scans from an $f = 3.05$ ML film of xenon on the second kish crystal. For $f = 3.05$ ML we find no evidence of a C phase for any of the xenon adsorbate at temperatures down to 46 K. These data do not correspond precisely to a longitudinal scan as such because they are taken at $Q_L = -0.1$ Å^{-1} so as to avoid the spurious $\lambda/3$ graphite (110) peak at the (Q_C, 0, 0) position. (b) Transverse rocks through the Q_{IC} peaks above. No significant variation in width is seen. We fit the $T = 103.1$ K data to three Lorentzians; this is consistent with a partial rotation of the adlayer by $0.41 \pm 0.03°$ at that temperature.

where the FCC stacking terms $S_{AB}(Q_L)$ and $S_{AC}(Q_L)$ span only two layers $n = 2.0$ of layer spacing a_0 in the bilayer case, and they are given by, for instance

$$S_{AB}(q_l) = [\sin(n\phi/2)/\sin(\phi/2)]^2 \tag{9}$$

where

$$\phi = (2\pi/3 + \sqrt{2/3}q_l a_0). \tag{10}$$

We interpret our modulated $f = 2.05$ ML results to indicate that above the IC–C transition the xenon adsorbate has a layered structure that corresponds qualitatively with the expectations from our volumetric measurements. That is, there is an approximately equal mix of the two energetically degenerate bilayer structures covering 85% of the surface the remainder being trilayer in form. These modulated multilayer data are quite distinct from the Bragg rod profile observed for the C component at 51.6 K in figure 8.

3.2. Trilayer behaviour

Figure 9(b) shows representative data taken by rocking the sample in plane and transversely to Q_H. At 103.1 K we see some evidence of a partial adlayer rotation by $\sim \pm 0.4°$. We sporadically observed small $\lesssim 0.5°$ partial rotations in our multilayer data, but we could not see the behaviour reproducibly. In one case of partial multilayer rotation we saw the effect appear at $\sim$ 85 K and the rotation angle decreased smoothly with decreasing temperature until it became truly aligned at around 55 K. Our observations of the effect were not reproduced, however, and we can make no definitive statements about adsorbate rotations. Hong [14] and Hamichi *et al* [20] report massive hysteresis for rotation effects in xenon super-monolayers $1 < f < 2$. In figure 9 we see that the mosaic of the unrotated trilayer xenon film is independent of temperature.

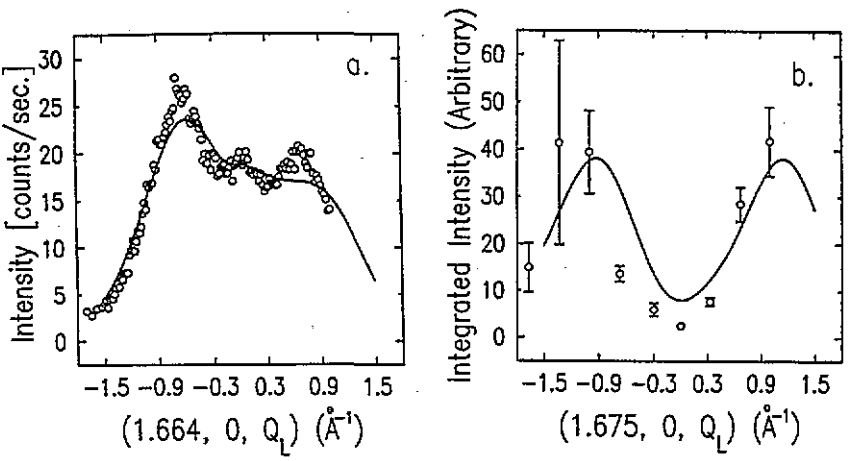

Figure 10. (a) $(Q_K,\ 0,\ Q_L)$ scan through the IC peak of the f = 3.05 ML film at 50.5 K and Q_{IC} = 1.664 Å. The model structure represented by the solid line is composed of four possible close-packed structures covering the following proportions of the substrate's surface: ABC, 38.2%, ACB, 25.0%, ABA, 18.4%, and ACA, 18.4%. (b) The variation in integrated intensity up and down the IC phase $(Q_K,\ 0,\ Q_L)$ scattering rod at 50.5 K. The solid line is the integrated intensity that would be expected for the structure proposed from the analysis in (a).

In figure 10 we present out of plane data from what we interpret to be a layered three-layer-thick structure. Figure 10(a) is a $(Q_{IC}, 0, Q_L)$ scan of the same type as that in figure 7. The data shown in figure 10(a) are inconsistent with expectations for a pure FCC structure in that they do not have a deep local minimum at $Q_L = 0$. Additionally there is no indication of peaks at $\sim \pm 1.3$ Å^{-1}. Likewise the data do not match with the scattering expected from a pure hexagonally close-packed (HCP) system in that they do not have strong local maxima at $\sim \pm 1.1$ Å^{-1}. Just as in the case of the f = 2.05 ML data, we estimate the Xe–Xe out of plane interlayer spacing at the temperature of study. The solid curve in figure 10(a) represents our expected rod scan profile for a structure that is constrained to relax only slightly by (2.7%) from our calculated estimate. The model is composed of various three-layer-thick domains each of which may be stacked ABC, ACB, ABA or ACA. In performing a fit to the relative proportions of the stacking sequences we find that all occur with essentially random relative frequencies. As the interactions that favour FCC structures over HCP in bulk xenon are very weak second-nearest-neighbour interactions, we are not surprised that in a film only three layers thick such effects do not appear to play a role. In performing the fit discussed, our trilayer structure factor has the form

$$(Q_{H0}, Q_L) \propto \int\int \mathrm{d}q_l\,\mathrm{d}q_h \Bigg(R[(q_h - Q_{H0}), (q_l - Q_L)] \frac{1}{1 + (q_h - Q_{H0})^2/\kappa_H^2} \mid f_{Xe}(q_l) \mid^2 \times \left[S_{ABC}(q_l) + S_{ACB}(q_l) + S_{ABA}(q_l) + S_{ACA}(q_l)\right] C(q_l) \Bigg) \tag{11}$$

where, for instance

$$S_{ABA}(q_l) = 3 + 2\cos(2\pi/3 + \sqrt{2/3}q_l a_0) + 2\cos(2\sqrt{2/3}q_l a_0) + 2\cos(2\pi/3 - \sqrt{2/3}q_l a_0). \tag{12}$$

In figure 10(b) we present out of plane data obtained by a different technique. This panel is generated by considering the evolution of the scattering rod's integrated intensity in

the (Q_H, Q_K) plane as a function of the distance up the rod Q_L. In figure 10(b) we scanned in the Q_H direction and the perpendicular $-Q_H + 2Q_K$ direction for each data point of a given Q_L. The intensity value is given by the product of the two Lorentzian widths and the peak amplitude. The data are corrected for the decrease with Q_L of the projected height of the resolution ellipsoid in the Q_L direction. There is also the illumination correction $C(Q_L)$ discussed earlier.

The solid curve in figure 10(b) is the integrated intensity behaviour we would expect for the model structure proposed in figure 10(a). The significant difference in the form of the actual data between the two parts of figure 10 demonstrates the dramatic influence of the resolution effects discussed earlier in reference to our Bragg rod scans. Both parts of figure 10 suggest that there is a qualitative agreement between our proposed model and the observed data. Our principal observation is that each of the four trilayer stackings occurs in random relative proportions each occuring in three layer thick domains on various parts of the substrate. This is complementary to the conclusion of Hong and Birgeneau [15] that the thicker multilayers are themselves stacked in a disordered manner within a given in plane domain. It is clear that as one goes to multilayers of thickness greater than a trilayer the cumulative effects of various stacking disorders render structural analysis difficult from a single Bragg rod.

3.3. Behaviour of thicker multilayers

In figure 11 we present longitudinal Q_H scans and transverse rocks through the IC peak of a six-layer ($f = 5.82$) film of xenon on high-quality single crystal graphite. For $Q = 1.665$ Å^{-1}, for instance, the overlayers are less dense than the $\sqrt{3} \times \sqrt{3}R30°$ C sites ($Q_C = 1.7055$ Å^{-1}) and so the number of atoms defined by $f = 5.82$ ML would correspond to an actual layered structure of ~ 6.18 layers.

(b) Transverse rocks through the longitudinal data peaks shown in (a). We note that the transverse width within a given data run appears to be approximately constant and yet there can be a significant variation in widths between one data run and the next.

We show representative scans from two independent cooling runs, which were absolutely reproducible in terms of their longitudinal behaviour. Their in plane mosaicity, however, differed dramatically as is shown in figure 11, although within a given cooling run the mosaicity was found to be approximately invariant with temperature. The peak amplitude varied between runs consistent with the transverse broadening. Related differences in adsorbate behaviour have been reported previously for monolayer rare gases on graphite [26]. This behaviour is thought to be related to the experimental rate of cooling as the system entered the solid phase from the high-temperature aligned liquid or 'hexatic' phase. Also in figure 11(a) we see once again the broadening of the longitudinal Q_H peak with decreasing incommensurability. By 45.9 K the peak is still substantially narrower in Q_H than its incommensurability and no transition to the C phase is seen to occur.

In figure 12 we present a figure for the thicker multilayers analogous to figure 5 for the bilayer. From this we see a far smaller contraction of the xenon overlayer with temperature and there is no indication of an IC–C transition. Data collection was initiated after allowing a period of approximately 90 min to elapse for equilibrium to be established.

Previous studies by Hong and Birgeneau [15] report a clear C phase for xenon multilayers of three or more layers on a large natural crystal of graphite, without significant difficulties arising from slow kinetics. Our larger surface length scale appears to lead to significantly slower low-temperature kinetics and longer equilibriation times. We took great care to ensure that our system was always in complete equilibrium but this nonetheless represents a serious concern. Despite our extreme care we see signs that the data for the trilayer system

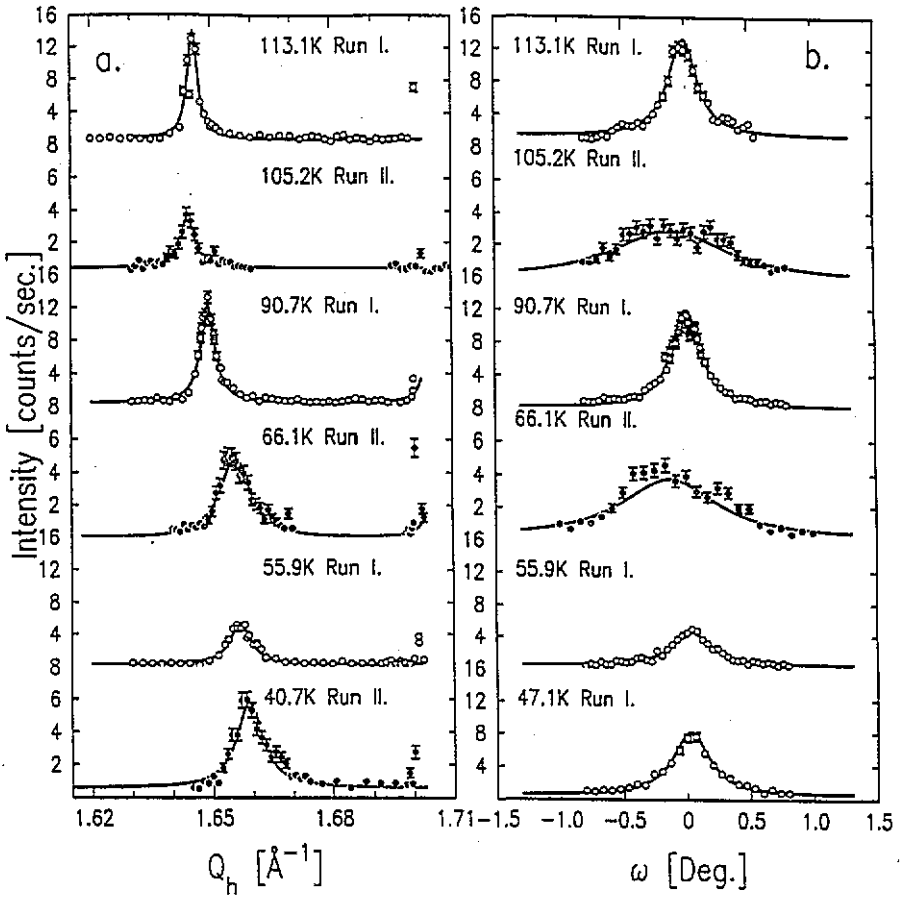

Figure 11. (a) Scattering profiles in the longitudinal (Q_H, 0, 0) direction for an f = 5.82 ML film of xenon on the second high-quality kish single crystal of graphite. Results from two data collection runs are shown: ○ from the first data run and ● from our repeated run. The sharp feature at $Q_H = Q_C \simeq 1.7055$ Å^{-1} is a residual signal from the $\lambda/3$ harmonic in the synchrotron energy distribution scattering from the (110) planes of the graphite substrate. We saw no sign of a C xenon structure for our six-layer film.

may have been insufficiently equilibriated because, for instance, the scattering vector for the in plane IC peak shifted by 0.011 Å^{-1} during the lengthy process of the rod scan and the integrated intensity measurement. We believe that the prohibitively slow kinetics of the thicker xenon multilayers adsorbed on very-high-quality substrates at low temperature may be the principal limit for experiments of this type. Additionally, the inferior substrate quality in the earlier studies may itself have favoured a partial C phase in the xenon multilayer and so observations from such a system could not be said to represent the physics of an ideal multilayer xenon–graphite system. Evidence for the effects of substrate surface morphology on the favourability of the xenon $1 < f < 2$ C phase is referred to by Mowforth *et al* [26] in explaining their x-ray diffraction observations. It appears, however, that their observations would also be consistent with an insufficiently equilibriated system [26].

From figure 12 we also note that for $63 < T < 115$ K the coefficient of linear thermal

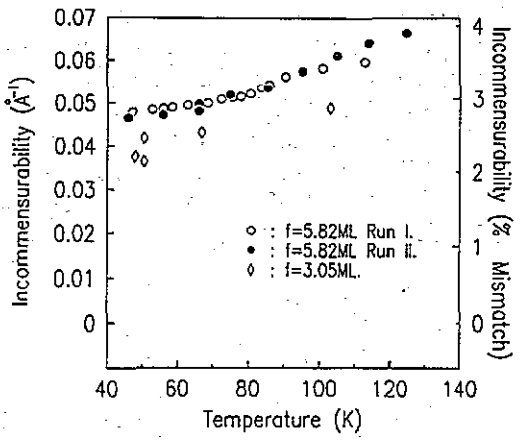

Figure 12. Incommensurability as a function of temperature for the $f = 5.82$ ML and the $f = 3.05$ ML films of xenon on graphite. No C xenon signal was seen for these systems. Note the two observed incommensurabilities of the 3.05 ML film at 50.5 K. Our out of plane studies in figure 10 were taken on these two distinct incommensurabilities on two separate cooling runs.

expansion of the six-layer xenon adsorbate is $\sim 1.7 \times 10^{-4}$ K^{-1}, which is slightly less than the value calculated from a fit to the bulk xenon data of Klein and Venables [25].

4. Conclusions

We have presented the results of a high-resolution synchrotron x-ray diffraction experiment to study the low-temperature structural properties of multilayer xenon films on a high-quality-single-crystal graphite substrate. Coverages of two, three and six monolayers were examined.

For a bilayer xenon film we see evidence of a two-layer-thick IC structure at high temperature that undergoes a first-order transition at 62.0 ± 1.2 K to a system with a C $\sqrt{3} \times \sqrt{3}$ $R30°$ component. We provide evidence that each of the C and IC components is a monolayer, and we conclude that the layer nearest to the graphite substrate has undergone a first-order phase transition to a C phase.

We observe that the bilayer system undergoes an IC–C transition when its incommensurability is of the same order as its longitudinal peak width, which broadens on cooling. This matches previous observations in the krypton monolayer system. We note that for the thicker multilayers we do not approach such a regime in the temperature range studied. We show that a three-layer and a six-layer xenon adsorbate do not undergo a phase transition to a structure with a C component for $T \gtrsim 45$ K.

In addition, we discuss the extremely slow kinetics of xenon adsorbates at low temperatures on kish substrates and emphasize the difficulties in ensuring system equilibrium in investigations of this type. We show that these multilayer films are not FCC and are instead what is best described as 'random close-packed stackings'. In particular, we believe the trilayer system to be composed of a great many in plane domains with linear dimensions of approximately 500 Å, each one of which may have ABC, ACB, ABA or ACA stacking.

We demonstrate the power of four-circle x-ray diffraction techniques, coupled with high-quality single-crystal substrates, in probing the structural phase behaviour of these technically challenging systems and look forward to relating our observations to the various pieces of information obtainable by other means.

Acknowledgments

We are most grateful to John Hill and Hawoong Hong for valuable discussions and technical assistance. We thank Kenneth Blum, Qiang Feng, Joan Harris, Brian McClain

and Do Young Noh for assistance during the synchrotron experiments. Do Young Noh also provided help with the data analysis. We should like to thank Jean Jordan-Sweet and René Holaday for their assistance at the MIT–IBM synchrotron facility and we acknowledge John Hill and others for the construction of the X20-B beamline. We thank E L Shaw and J R Martin of the Surface Analysis Facility at MIT. One of us (WJN) gratefully acknowledges the financial assistance of SERC (UK). This work was supported by the Joint Services Electronics Program under contract No DAAL03-92-C-0001. The National Synchrotron Light Source is supported by the US Department of Energy under contract No DEAC0276CH00016.

References

[1] Birgeneau R J and Horn P M 1986 *Science* **232** 329
[2] Kariotis R, Venables J A, Hamichi M and Faisal A Q D 1987 *J. Phys. C: Solid State Phys.* **19** 5717
[3] Ashcroft N W and Mermin N D 1976 *Solid State Physics* (Philadelphia: Saunders College) p 70
[4] Hong H, Peters C J, Mak A, Birgeneau R J, Horn P M and Suematsu H 1989 *Phys. Rev.* B **40** 4797
[5] Hong H, Peters C J, Mak A, Birgeneau R J, Horn P M and Suematsu H 1987 *Phys. Rev.* B **36** 7311
[6] Villain J 1980 *Surf. Sci.* **97** 219
[7] Stephens P W, Heiney P, Birgeneau R J and Horn P M 1979 *Phys. Rev. Lett.* **43** 47
[8] Shrimpton N D, Joós B and Bergeson B 1988 *Phys. Rev.* B **38** 2124
[9] Coppersmith S N, Fisher D S, Halperin B I, Lee P A and Brinkman W F 1982 *Phys. Rev.* B **25** 349
[10] Bak P, Mukamel D, Villain J and Wentowska K 1979 *Phys. Rev.* B **19** 1610
[11] Caflisch R G, Berker A N and Kardar M 1985 *Phys. Rev.* B **31** 4527
[12] Kariotis R, Venables J A and Prentis J J 1988 *J. Phys. C: Solid State Phys.* **21** 3031
[13] Bruinsma R and Zangwill A 1987 *Europhys. Lett.* **4** 729
[14] Hong H 1988 *PhD Thesis* Massachusetts Institute of Technology
[15] Hong H and Birgeneau R J 1989 *Z. Phys.* B **77** 413
[16] Hamichi M, Faisal A Q D, Venables J A and Kariotis R 1989 *Phys. Rev.* B **39** 415
[17] Faul J W O, Volkmann U G and Knorr K 1990 *Surf. Sci.* **227** 390
Ser F, Larher Y and Gilquin B 1989 *Mol. Phys.* **67** 1077
[18] Fahey K P 1992 *BS Thesis* Massachusetts Institute of Technology
[19] Hill J P, Nuttall W J and Hong H 1990 *National Synchrotron Light Source Annual Report* p 310
[20] Hamichi M, Kariotis R and Venables J A 1991 *Phys. Rev.* B **43** 3208
[21] Stephens P W, Heiney P A, Birgeneau R J, Horn P M, Moncton D E and Brown G S 1984 *Phys. Rev.* B **29** 3512
[22] Mandel T, Domke M and Kaindl G 1988 *Surf. Sci.* **197** 81
[23] Fain S C Jr, Chinn M D and Diehl R D 1980 *Phys. Rev.* B **21** 4170
[24] Sandy A R 1992 *PhD Thesis* Massachusetts Institute of Technology
[25] Klein M L and Venables J A 1986 *Rare Gas Solids* (London: Academic)
[26] Mowforth C W, Rayment T and Thomas R K 1986 *J. Chem. Soc. Faraday Trans* II **82** 1621